UW Journal of Science and Technology Vol. 5 (2021) 20-27
ISSN: 2523-0123 (Print) 2616-4396 (Online)

University of Wah
Journal of Science and Technology

www.uow.edu.pk

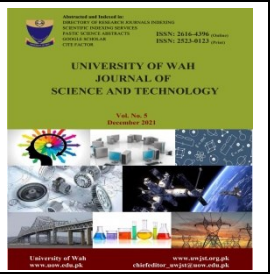

Robust Control of Gimbal Based Robotic Eye for Humanoid Robots

Atif Mahmood 1*, Abdul Qayyum Khan 1, Ghulam Mustafa 1, Muhammad Abid 1, Tahir Ejaz 2, Muhammad Asim Shoaib 1

***Abstract*-- In the current age of automation, robots have been designed to interact and work with humans. Humanoid robots are mostly used for this social interaction. To interact in a social environment, robots need high decoupling of a camera sensor from the head skeleton to point, track and recognize the stimuli. This high decoupling of a camera sensor from the head skeleton is easily achieved by using the decoupling property of a gimbal system. To further increase the tracking performance, we estimate the friction disturbance torque and then compensate it using MATLAB/SIMULINK. We addressed the frictional disturbance torque in both the channels of the gimbal system using observer-based controller design and stabilize the gimbal-based robotic eye. To show the Saccade like the human eye, we performed simulations for tracking control. The designed controller is robust against frictional disturbance. The simulation results illustrate the stabilization and tracking control of the gimbal-based robotic eye and the estimation and compensation of frictional disturbance. This will be a valuable step towards humanoid robots.**

***Index Terms*--**Robotic vision system; decoupling; stabilization control; frictional disturbance; gimbal system

Manuscript received: September 14, 2021; Accepted: December 27, 2021

Atif Mahmood 1*, Abdul Qayyum Khan 1, Ghulam Mustafa 1, Muhammad Abid 1, Tahir Ejaz 2, Muhammad Asim Shoaib 1
Atif Mahmood*, Abdul Qayyum Khan, Ghulam Mustafa, Muhammad Abid, Muhammad Asim Shoaib
Department of Electrical Engineering, Pakistan Institute of Engineering and Applied Sciences, Nilore, Islamabad.
Tahir Ejaz, Grafton College of Engineering & Sciences, Park link Rd, Islamabad.
Email Ids: engg.khaki@gmail.com, aqkhan,gm,mabid)@pieas.edu.pk, tahir.ejaz@pk.graftoncollege.org. asim_930@yahoo.com

Corresponding Author : Atif Mahmood (engg.khaki@gmail.com)

I. Introduction

FOR communication with humans or with other robots in a human-robot community, robots need quick eyeball movement. The quick eyeball movement helps in the perception of more information about a target like a human perceives more than 80 percent of information through the eyes [1]. In a competitive environment, the perception of more information is essential for the survival of the fittest. To get more information about a target, researchers have worked a lot on robotic eyes.

Taking the optimal human eye is as a reference, researchers worked on the brain/decision making, extra-ocular muscles/actuators of the camera sensor, and eyeball/camera in the last 20 years. For example, some robotic communities worked on Artificial Intelligence (AI) based brain/vision controller includes i.e., tracking algorithms, scanning algorithms, and recognition algorithms [3-5]. To model the actuators of the eyeball, few researchers used a pneumatic control system [6] or soft pulleys [7-9] but the problem was a slow movement that can't track a fast stimulus in a dynamic world due to low decoupling with robotic head. Some the researcher worked on the eyeball and use movable cameras [10-13]. This idea reduced the decoupling with head skeleton but still unable to work in a human environment where walking or sudden change of direction may require. An excellent effort is done in [14] to further reduce the decoupling of an eyeball with a robotic head skeleton. The authors used the decoupling property of a gimbal system and proved that the gimbal-based robotic eye has fewer viewpoint changes than the existing robotic eyes. The authors tested vestibular ocular reflex (VOR)-based movement on Zenmuse-X3 gimbal camera relative to pre-defined YAW movements of the DJI Matrice-100 unmanned aerial vehicle (UAV). A similar effort is done in [15] using a gimbal system for the robotic eye.

In the aforementioned research, the disturbances of gimbal systems are not considered that affect the tracking

performance. The idea of using a gimbal system in a robotic eye for humanoid robots is explained in more detail in the reference [2] with similarities between the human eyeball and the gimbal-based robotic eye. The authors proved that the gimbal system helps in coordination among the eyeball movement, vision controller, and actuators by providing a high decoupling ratio. Apart from the advantages of using the gimbal system in a robot eye, the gimbal system itself faces problems when used in a robot eye. These problems are due to the mass imbalances, frictional disturbance in the pitch and yaw channels, and the jerks due to robot movement in the circumstances like walking, riding, or sudden change of direction, etc. in a social environment. If we minimize or decouple these disturbances of the gimbal system for the robotic eye, the eyeball will move more smoothly that will further minimize the viewpoint changes. This in turn results in smooth and efficient target tracking for the perception of more information. For this purpose, a robust controller is required that decouple the disturbances and maintain smooth tracking. The mathematical equations will help in the identification of disturbances that affect the tracking performance and the control design will be responsible for the decoupling and minimization of disturbance and controlled movement of the robotic eye. The research in hand provides both the mathematical equations and identification of disturbance and a robust controller for a gimbal-based robotic eye with the following contribution.

1. After we identified the frictional disturbances in gimbal based robotic eye, we estimate and compensate the frictional disturbances in both the pitch and yaw channels.
2. We design an observer-based stabilizing control as observer-based control has excellent response where system dynamics are available. The controller is robust against frictional disturbances.
3. To demonstrate the Saccade like human eye, we simulate the system for tracking reference signals.

The remaining sections of the paper are divided into the following sections: Section II includes the complete problem formulation by starting with the introduction of Lie algebra of a real human eyeball movement. Section III presents the controller design and in section IV we include some simulation results and then concluded the paper.

Table 1
Symbols used

Symbol	Meaning To Robotic Eye
B	Body-fixed Frame
K	Yaw channel Frame
A	Pitch channel Frame
p q r	Angular velocity components of frame B
p_k q_k r_k	Angular velocity components of Frame K
p_a q_a r_a	Angular velocity components of Frame A Outputs of control system for stabilization
v_1/Θ	Angle of rotation of Yaw channel
v_2/ψ	Angle of rotation of Pitch channel
J	Moment of inertia
D	Product of inertia for Pitch channel with appropriate indices
d	Product of inertia for Yaw channel with appropriate indices
T_y	Total external torque about the pitch channel
T_z	Total external torque about the yaw channel

II. MATHEMATICAL MODELING

A. Saccade and Lie Algebra of Real Human Eyes

A quick movement of an eye for bringing a target into the center of the visual field is called a saccade. The saccade is required for fast stimulus tracking or working in a dynamic environment. The automatically possible positions restrict the eye position during movement to a subset. Donder's law states that "the gaze direction of the eye determines its orientation uniquely, and the orientation is independent of eye motion history that leads to gaze direction". The observed orientation of the eyes is the one that can be reached from the primary position via a single rotation about an axis that is in a plane perpendicular to the gaze direction. Listing law precisely specifies the allowed space of position.

The three-dimension group, $G=SO_3$ [16] (Special Orthogonal Transformation [17]) of rotation is used to describe both the actual rotation and its unique virtual rotation from the primary position. We use the identity operation to retain the eye at a primary position with the unit element of the group $e \in SO_3$. A 3D axis and angle of rotation can parameterize a rotation. By increasing the angle, a continuous set of rotations can be generated for each axis. If we take "n" as a unit axis of rotation, then $\exp(\psi.n)$ is a continuous one-parameter subgroup

$SO_2 \subseteq SO_3$ of rotation through angle ψ in the plane that is perpendicular to n. The calculation of exponent and explicit representation of n as a matrix can be done using the Taylor series expansion. For example, at the one parameter of a subgroup of rotation in x-y plane, i.e. about z-axis

representation of matrix case is Now the rotation by an angle ψ via direct computation gives

$$\exp(\psi L_z) = I + \psi L_z + \frac{1}{2!}(\psi L_z)^2 + ... + \frac{1}{n!}(\psi L_z)^n + ... \quad ...(1)$$

$$\exp(\psi L_z) = \begin{bmatrix} \cos\psi & \sin\psi & 0 \\ -\sin\psi & \cos\psi & 0 \\ 0 & 0 & 1 \end{bmatrix} \quad L_z = \begin{bmatrix} 0 & 1 & 0 \\ -1 & 0 & 0 \\ 0 & 0 & 0 \end{bmatrix}$$

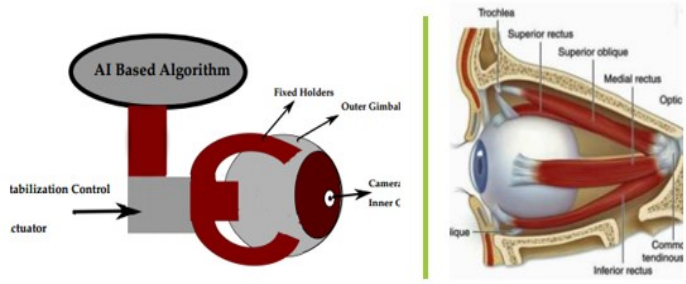

Figure 1: The human eye and gimbal based robotic eye

B. The Human Eye and Gimbal Based Robotic Eye

A detailed discussion on the human eye and gimbal-based robotic eye is given in [2]. We need the mathematical resemblance in the eyeball/camera sensor's movement. The Lie algebra of the human eye is discussed in subsection A where the dynamic equations of motion of the gimbal system are given in [18]. The authors performed the transformation of Fixed-Body to the yaw channel and the yaw channel to pitch channel using the following transformation.

$$L_{KB} = \begin{bmatrix} \cos\nu_1 & \sin\nu_1 & 0 \\ -\sin\nu_1 & \cos\nu_1 & 0 \\ 0 & 0 & 1 \end{bmatrix}$$

$$L_{AK} = \begin{bmatrix} \cos\nu_2 & 0 & -\sin\nu_2 \\ 0 & 1 & 0 \\ \sin\nu_2 & 0 & \cos\nu_2 \end{bmatrix}$$

We have used Θ instead v1 and ψ instead v2. The dynamic equations of motion for both gimbals are derived along with complete analysis. We will use these equations of motion to analyze the disturbance and then estimation and compensation of disturbances to improve the tracking performance.

C. Equations of Motion:

The equations of motions for the pitch and yaw channels are derived in [18] that are given below.

1) Equation of Motion for Yaw Gimbal

The equation of motion of yaw gimbal or outer channel is derived using equation 7, that is:

$$\ddot{\psi} = \frac{1}{J_{kz} + \cos^2\theta - \sin^2\theta}[T_z - [J_{ax}P_a\cos\theta + J_{az}r_a\sin\theta + \cos\theta(P_k\cos\theta - r_k\sin\theta) - \sin\theta(P\cos\psi + q\sin\psi) - r\cos\theta]\dot{\theta} - (\cos\theta\sin\theta)\dot{\theta}\dot{\psi} - \cos\theta[\sin\theta(q\cos\psi - P\sin\psi)]\dot{\psi} - (J_{kz} - \sin^2\theta)\dot{r} - [\dot{P}\cos\theta\sin\theta + \dot{q}(\sin\theta\sin\psi) + \dot{r}\cos\theta]\cos\theta] + P_k q_k(J_{ky} - J_{kx}) + P_a q_a J_{ay} - P_a q_k J_{ax}\cos\theta - q_k r_a J_{az}\sin\theta \quad ...(2)$$

2) Equation of Motion for Pitch Gimbal:

Similarly, dynamic equation of motion for pitch gimbal or pitch channel is obtained using equation (7) as below:

$$\ddot{\theta} = \frac{1}{J_{ay}}[T_y + (J_{ky} - J_{ay})(\dot{q}\cos\psi - \dot{p}\sin\psi) - J_{ax}P_a(P\sin\theta + r\cos\theta) - J_{az}r_a(P\cos\theta - r\sin\theta) - J_{kx}P_k r - J_{kz}Pr_k] - \frac{1}{J_{ay}}[(J_{ky} - J_{ay})(P\cos\psi - q\sin\psi)\dot{\psi}] \quad ....(3)$$

Where,

$$p_k = p\cos\psi + q\sin\psi \qquad p_a = p_k\cos\theta - q_k\sin\theta$$
$$q_k = -p\sin\psi + q\cos\psi \qquad q_a = q_k + \dot{\theta}$$
$$r_k = r + \dot{\psi} \qquad \text{and} \qquad r_a = -p_k\sin\theta + q_k\cos\theta$$

D. Disturbances Estimation and Compensation in Both Channels

Analysis of the equations reveals that the equations for both pitch and yaw channels are consisted of rotating torque and disturbance torques. The block diagram of the yaw and pitch channel can be shown in Figures 2, 3. There are two types of torque on the yaw channel that are external torque and disturbance torque. The external torque rotates the yaw channel about the z-axis while the disturbance torque is due to inertial effects. A well-known fact and terminology called frictional torque are caused when two objects are in contact move. This frictional torque may be measured in Newton-meter in SI system like other torques. This fact needs to be considered in modeling the gimbal system. The frictional torque resists the rotational movement and exerts force in the opposite direction. Friction is among the most unwanted disturbances that decrease the tracking performance and cause a steady-state error. Being control engineers, we must always aim to minimize it. Here static friction is considered that occurs in the bearing of both channels during its pointing and tracking process. This frictional force can be minimized to improve the tracking performance of the gimbal-based robotic eye. To mathematically model the frictional torque, we consider static frictional disturbance that can be written as

$$T_{ky} = C_Z\dot{\psi} \quad ...(4)$$

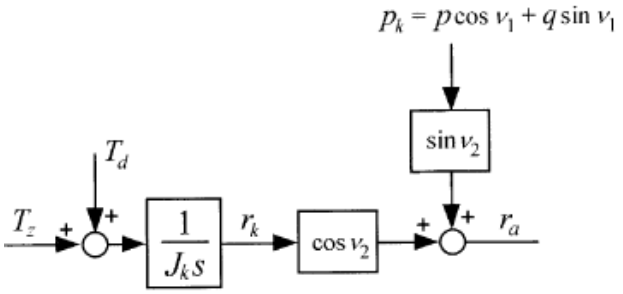

Figure 2: Block diagram of Yaw Channel

T_{ky} is total frictional torque at the yaw channel rotating about the negative Z_i-axis, C_z is the magnitude of friction, and $\dot{\psi}$ is the angular rate at which it rotates. The dynamic equations of motion for the yaw channel with frictional disturbances can be written as below.

$$\ddot{\psi} = \frac{1}{J_{kz} + \cos^2\theta - \sin^2\theta}[T_z - [J_{ax}P_a\cos\theta + J_{az}r_a\sin\theta + \cos\theta(P_k\cos\theta - r_k\sin\theta) - \sin\theta(P\cos\psi + q\sin\psi) - r\cos\theta]\dot{\theta} - (\cos\theta\sin\theta)\dot{\theta}\dot{\psi} - \cos\theta[\sin\theta(q\cos\psi - P\sin\psi)]\dot{\psi} - (J_{kz} - \sin^2\theta)\dot{r} - [\dot{P}\cos\theta\sin\theta + \dot{q}(\sin\theta\sin\psi) + \dot{r}\cos\theta]\cos\theta] + P_k q_k(J_{ky} - J_{kx}) + P_a q_a J_{ay} - P_a q_k J_{ax}\cos\theta - q_k r_a J_{az}\sin\theta + C_Z\dot{\psi} \quad \ldots(5)$$

The block diagram in Figure 2 of the yaw channel with frictional disturbance is given as.

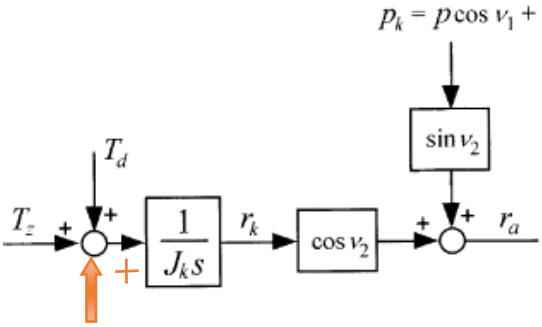

Figure 3: Block diagram of Yaw channel with frictional disturbance

Similarly, the block diagram of pitch channel is show in figure 4.

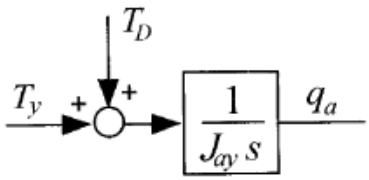

Figure 4: Block diagram of Pitch Channel

Figure 4 clearly shows that there are two types of torque working on the pitch channel that are external torque and disturbances torque. The external torque rotates the pitch channel about the y-axis while the disturbance torque is due to the inertial effect. There also exists frictional torque that forces the channel in a reverse direction and resists the rotation. This frictional torque can be shown as a block diagram as shown in Figure 5.

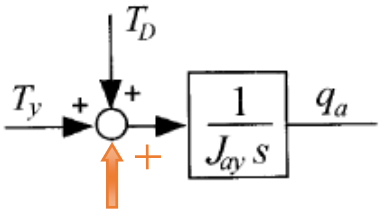

Figure 5: Pitch channel with frictional disturbance

Mathematical the static frictional disturbance can be written as [20]

$$T_{ap} = C_y\dot{\theta} \quad \ldots(6)$$

Here, T_{ap} is total frictional torque at the pitch channel rotating about y_i-axis, C_y is the magnitude of friction and $\dot{\theta}$ is the angular rate at which it rotates. The dynamic equations of motion for both gimbals with frictional disturbances can be written as

$$\ddot{\theta} = \frac{1}{J_{ay}}[T_y + (J_{ky} - J_{ay})(\dot{q}\cos\psi - \dot{p}\sin\psi) - J_{ax}P_a(P\sin\theta + r\cos\theta) - J_{az}r_a(P\cos\theta - r\sin\theta) - J_{kx}P_k r - J_{kz}Pr_k] - \frac{1}{J_{ay}}[(J_{ky} - J_{ay})(P\cos\psi - q\sin\psi)\dot{\psi}] + C_y\dot{\theta} \quad \ldots(7)$$

Remark 1: The two outputs q_a and r_a of the control systems for stabilization can be calculated by using body-fixed rate gyros for the two angles v1 and v2.

E. Learization and State Space Representation

The two equations of motion (5), (7) are nonlinear and cross coupled so complex to analyze and control. Complete details of the equations are given in [18]. We convert the two nonlinear equations into 4 linear equations by linearization. This

linearization is carried out at singular point (0,0,0,0) at the origin using Jacobian and Taylor methods. The reason for linearization about the origin is that each equilibrium point can be shifted to origin with the change of variables without the loss of generality. The state parameters are the position and velocities of pitch and yaw channels that are $\psi, \dot{\psi}, \theta, \dot{\theta}$ ψ and two outputs that are position of pitch and yaw channels $\psi$and θ. The ui is the input to the pitch channel that will rotate it. Similarly, uo is the input to the yaw channel. The final state-space equations are given below.

$$\dot{x(t)} = Ax(t) + Bu(t)$$
$$y = Cx(t) + Du(t) \quad \ldots(8)$$

Where the matrices A, B, C, and D are given as

$$A = \begin{pmatrix} 0 & 1 & 0 & 0 \\ J_{kz}(P_a q + q^2 J_{ay} - q(J_{ky} - J_{kx})) & 0 & 0 & 0 \\ 0 & 0 & 0 & 1 \\ \frac{(J_{ky} - J_{ay})\dot{P}}{J_{ay}} - J_{kx} q r & \frac{(J_{ky} - J_{ay})P}{J_{ay}} & J_{kz}[J_{kz} P_k - q^2(J_{ky} - J_{kz}) + J_{az} r_a q_k] & 0 \\ & & \frac{J_{ax} P P_a}{J_{ay}} & 0 \end{pmatrix}$$

$$B = \begin{bmatrix} 0 & 0 \\ \frac{T_z}{J_{kz}+1} & 0 \\ 0 & 0 \\ 0 & \frac{Ty}{J_{ay}} \end{bmatrix} \quad C = \begin{bmatrix} 1 & 0 & 0 & 0 \\ 0 & 0 & 1 & 0 \end{bmatrix}$$ and D=0

Matrix A is the state matrix with states parameters $\psi, \dot{\psi}, \theta, \dot{\theta}$ that are the position and angular velocities of the outer gimbal and inner gimbal respectively. Matrix B is the input matrix or source agency that will rotate the channels of the gimbal system. The matrix C is the output matrix with two outputs that are the positions of pitch and yaw channels. As there is no direct connection to output, so the matrix D will lead to zero entries of appropriate size.

F. Stability Analysis

The two-axis gimbal system is an unstable mechanical system having two channels namely, pitch gimbal and yaw gimbal. The instability of the system can be seen from
the phase portrait plots of the nonlinear equations (5) and (7), derived via mathematical modeling.

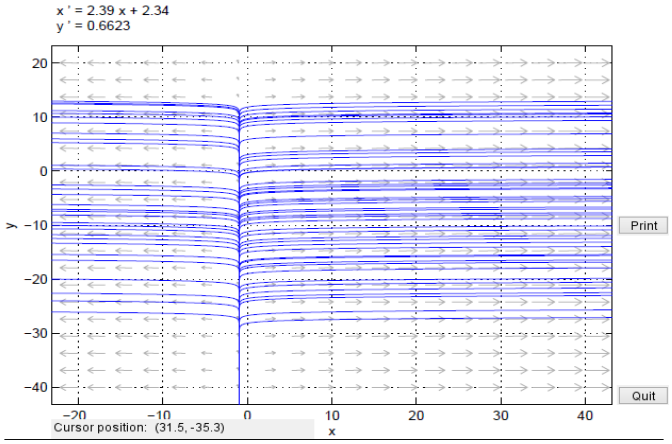

Figure 6: Phase portrait plot of the nonlinear equations

The instability is also conformed from the Lyapunov's method with the P matrix calculated computationally for steady state and also using MATLAB. The matrix P with eign values are given below

```
Eign values of P also prove the instability of the linearized Plant
P =
  -642.0000    0.5000    1.0000    0.6200
     0.5000    9.8800   -0.6200    1.0000
     1.0000   -0.6200  137.0000    0.5000
     0.6200    1.0000    0.5000    1.2700

EIG_P =
  -642.0023
     1.1535
     9.9927
   137.0061
```

The matrix P is asemi-negative definite matrix so according to Lyapunov theory the system is unstable. The nonlinear plant can be controlled after linearization about its equilibrium point. For this purpose, we design a controller using pole placement and connected in feedback which can stabilize the plant but is not tracking the reference step input perfectly as shown in Figure 7, demonstrates the instability of the linearized plant's states and also the stability of feedback-controlled states in (7b). K1 is the controller gain and A-BK eigen values are at the left half plane which ensure the stability of the controlled system but again with a larger steady-state error.

```
K_1 =
   -39.4788   -3.6924   -4.8985    0.2185
    -1.1133   -0.0084   -2.0842    0.1454

AA=A-B*K_1
         0    1.0000         0         0
  -14.7713   -7.7415    1.7299    0.4581
         0         0         0    1.0000
    1.5649    0.4177  -12.9784   -7.2585

EIG_Ac =
   -3.0000
   -4.5000
   -3.5000
   -4.0000
```

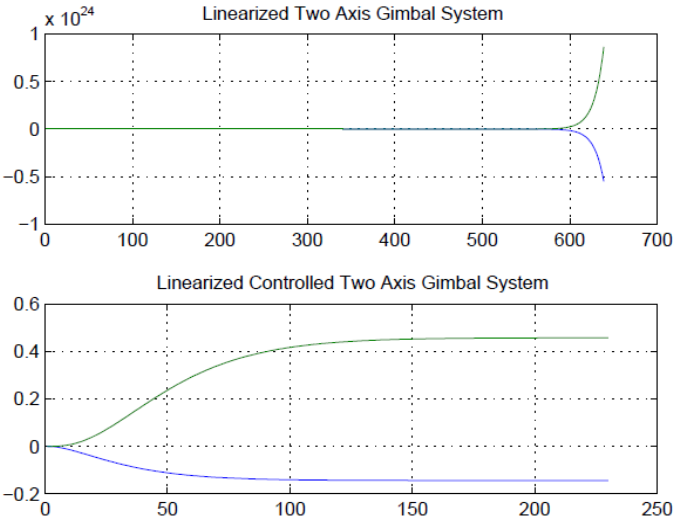

Figure 7: State response of linearized and controlled linearized system

III. Observer Based Control Design

We used an observer-based controller as it has best the response when all states are known. An observer comprises real-time simulations of the system, driven by the same data input of the plant and by a correcting term derived from the difference between the actual plant output and the predicted output of the observer. The state space description of the observer is given as:

$$\dot{\hat{x}} = A\hat{x} + Bu - L(y - \hat{y})$$
$$\hat{y} = C\hat{x} + Du \quad \ldots(9)$$

where L is the estimator gain, that estimates the disturbance and $\hat{x}$ and $\hat{y}$ is the estimated states and output respectively. The difference between plant output and observer output is called residual signal which in case of no disturbance has zero amplitude. The error vector is given by

$$\dot{e} = \dot{x} - \dot{\hat{x}}$$
$$\dot{e} = Ax + Bu - A\hat{x} - Bu + L(y - \hat{y})$$
$$\dot{e} = A(x - \hat{x}) + L(Cx - C\hat{x})$$
$$\dot{e} = (A + LC)e \quad \ldots(10)$$

The observer-based state feedback controller with frictional disturbance compensation consists of

- An observer:

$$\begin{bmatrix} \dot{\hat{x}} \\ \dot{\hat{d}} \end{bmatrix} = \begin{bmatrix} A & E_d \\ 0 & 0 \end{bmatrix} \begin{bmatrix} \hat{x} \\ \hat{d} \end{bmatrix} + \begin{bmatrix} B \\ 0 \end{bmatrix} u + L_e(y - C\hat{x}) \ldots(11)$$

- State feedback Controller:

$$u = -K\hat{x} - \hat{d} \quad \ldots(12)$$

- Estimator Gain

$$L_e = \begin{bmatrix} L_1 \\ L_2 \end{bmatrix} \quad \ldots(13)$$

L1 is the system's states estimator gain while L2 is the frictional disturbances states estimator gain. The block diagram of observer-based estimation and compensation process is given in figure (8).

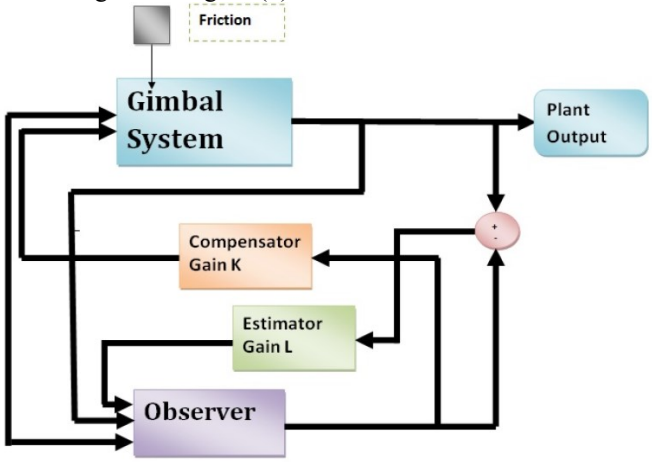

Figure 8: Observer-based control of gimbal based robotic eye

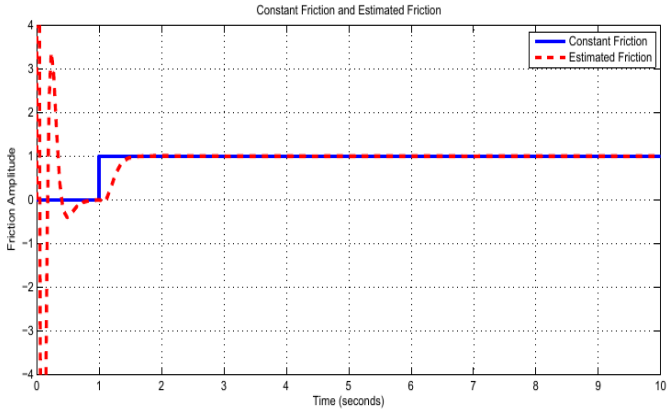

Figure 9: Estimation of frictional disturbance in gimbal

IV. Simulation Results

The simulations results for gimbal-based robotic eye are accomplished using MATLAB/SIMULINK. To show the estimation and compensation of frictional disturbance, we calculate the estimator and compensator gain using the pole placement method using MATLAB and then call both gain matrices to SIMULINK. The static frictional disturbance with estimated plots is given in figure (9) while the plant output with compensated friction is given in figure (10). The simulation results demonstrate the frictional disturbances estimation and compensation, and then the plant stabilization control. As mentioned in section II part A, a real human eye moves quickly to bring a stimulus in the center of the visual field, and the movement is called Saccade, we performed simulations for reference tracking in the presence of the frictional disturbance. For this purpose, we use step input and ramp input as a reference signal. The simulation results are done for both Yaw and Pitch channels given in figures (11) to (14). The tracking of reference input proves the Saccade and bringing of stimuli to the center of the visual field. All the states and gain matrices are given in Appendix.

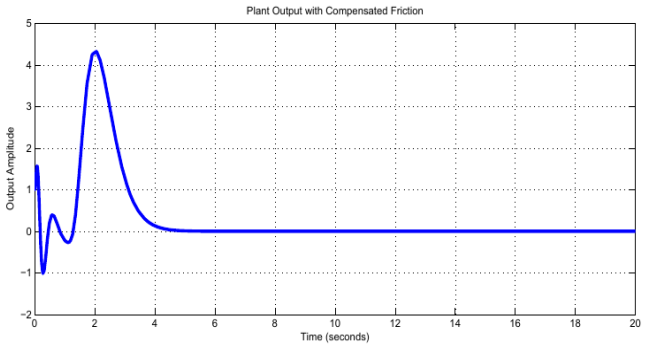

Fig. 10. Stabilization control of gimbal based robotic eye with compensated friction

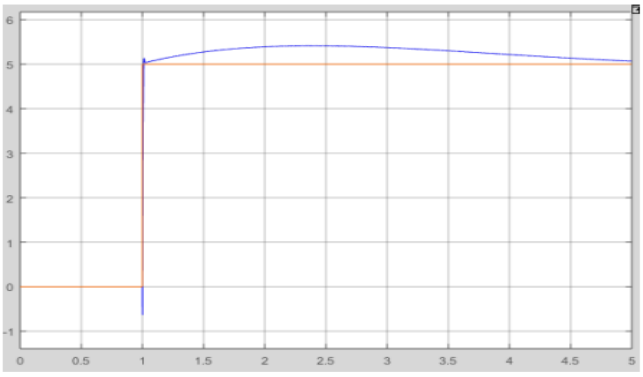

Figure 11: Response of Yaw channel for step input

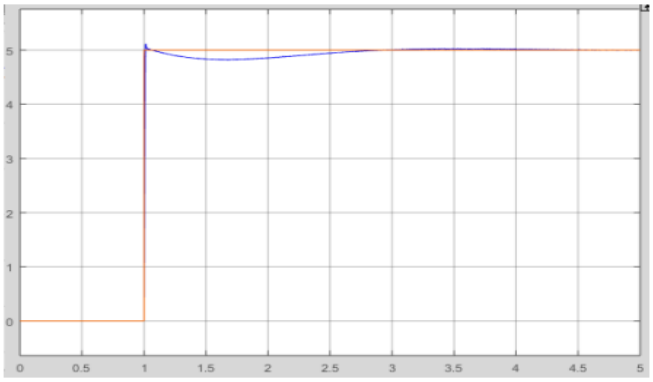

Figure 12: Response of Pitch channel for step input

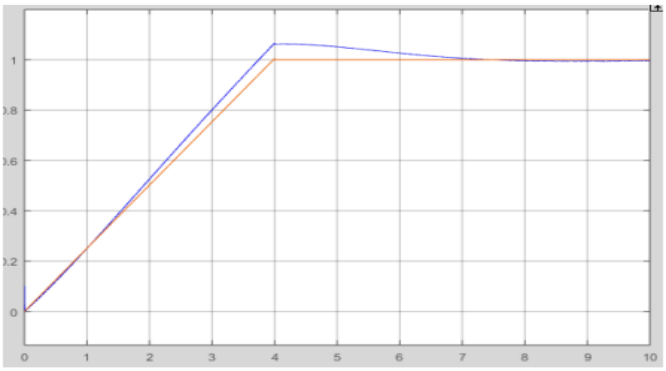

Figure 13: Response of Yaw channel for ramp input

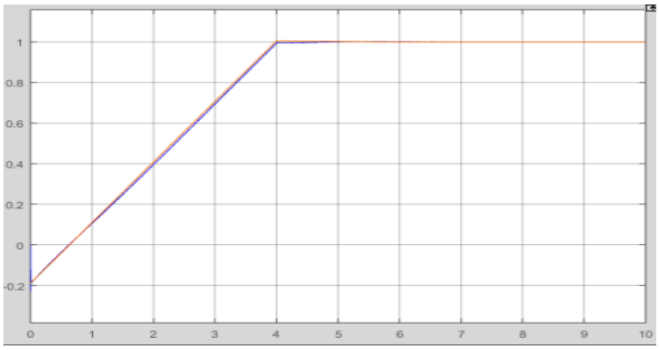

Figure 14: Response of Pitch channel for ramp input

V. Conclusion

In this work, we identify the frictional disturbances torque and address the process mathematically and by simulations. The additional disturbances are then estimated and compensated using the observer-based control design. The simulation results of observer-based control prove that the control is robust against frictional disturbances. To show the bringing of a target in the center of the visual field called saccade for a robotic eye, we have performed simulations for reference tracking. The strep reference and ramp reference inputs are perfectly tracked

using MATLAB/SIMULINK software. To further improve the tracking performance of gimbal-based robotic eyes, the static and dynamic mass imbalances can be minimized.

REFERENCES

[1] D. A. Forsyth and J. Ponce, A modern approach, Computer vision: a modern approach, pp. 88-101, 2003.

[2] A. Mahmood, A. Q. Khan, G. Mustafa, M. Abid, A. S. Khan and H. u. Rasheed, "Gimbal Based Robotic Eye for Dynamic Social Environment," 2020 International Symposium on Recent Advances in Electrical Engineering & Computer Sciences (RAEE & CS), 2020, pp. 1-5, doi: 10.1109/RAEECS50817.2020.9265725.

[3] W. Jang and Z. Bien, (1991) "Feature-based visual servoing of an eyein- hand robot with improved tracking performance", in Robotics and Automation, 1991. Proceedings., IEEE International Conference on, pp. 2254-2260, 1991.

[4] https://howtomechatronics.com/projects/diy-arduino-gimbal-selfstabilizing-platform/

[5] A. Manecy, J. Diperi, M. Boyron, N. Marchand, and S. Vi-ollet, "A novel hyperacute gimbal eye to implement precise hovering and target tracking on a quadrotor", in Robotics and Automation (ICRA), IEEE International Conference on, pp. 3212-3218, 2016.

[6] M. D. Kim and J. Ueda, "Dynamics-based motion de-blurring improves the performance of optical character recognition during fast scanning of a robotic eye", IEEE/ASME Transactions on Mechatronics, 2018.

[7] C. L. Choi, J. Rebello, L. Koppel, P. Ganti, A. Das and S. L. Waslander, "Encoderless Gimbal Calibration of Dynamic Multi-Camera Clusters," 2018 IEEE International Conference on Robotics and Automation (ICRA), 2018, pp. 2126-2133, doi: 10.1109/ICRA.2018.8462920.

[8] A. Manecy, J. Diperi, M. Boyron, N. Marchand and S. Viollet, "A novel hyperacute gimbal eye to implement precise hovering and target tracking on a quadrotor," 2016 IEEE International Conference on Robotics and Automation (ICRA), 2016, pp. 3212-3218, doi: 10.1109/ICRA.2016.7487490.

[9] S. Huber, B. Selby and B. P. Tripp, "Design of a Saccading and Accommodating Robot Vision System," 2016 13th Conference on Computer and Robot Vision (CRV), 2016, pp. 350-357, doi: 10.1109/CRV.2016.48.

[10] Difference between a gimbal, the human eye and in camera stabilization, https://www.youtube.com/watch?v=ButbHMqUDuA, Oct 13, 2017.

[11] C. Gielen, S. Gabel, and J. Duysens, "Retinal slip during active head motion and stimulus motion", Experimental brain research, vol. 155, no. 2, pp. 211-219, 2004.

[12] S. Schulz, I. Lutkebohle, and S. Wachsmuth, "An affordable, 3dprintable camera eye with two active degrees of freedom for an anthropomorphic robot", in Intelligent Robots and Systems (IROS), IEEE/RSJ International Conference on, pp. 764-771, IEEE, 2012.

[13] D. Pongas, F. Guenter, A. GuIgard, and A. G. Billard, "Development of a miniature pair of eyes with camera for the humanoid robot" 4th IEEE/RAS International Conference on, vol. 2, pp. 899-911, IEEE, 2004.

[14] Cunha, Rita and Malaca, Miguel and Sampaio, "Gimbal control for vision-based target tracking, Proceedings of the European Conference on Signal Processing, 2019.

[15] Chai, Young Ho and Patil, Ashok Kumar, "Inspired by human eye: Vestibular ocular reflex based gimbal camera movement to minimize viewpoint changes", Symmetry, vol 11, no, 1, 2019.

[16] A. A. Handzel and T. Flash, "The geometry of eye rotations and listing's law", in Advances in Neural Information Processing Systems, pp. 117-123, 1996.

[17] R. Gilmore, Lie groups, "lie algebras and some of their representations", Mathematics of the USSR-Izvestiya ,1974.

[18] B. Ekstrand, "Equations of motion for a two-axes gimbal system," in *IEEE Transactions on Aerospace and Electronic Systems*, vol. 37, no. 3, pp. 1083-1091, July 2001, doi: 10.1109/7.953259

[19] R. Gilmore, Lie groups, "lie algebras and some of their representations", Mathematics of the USSR-Izvestiya ,1974.

[20] A. Q. Khan, Observer based fault detection in nonlinear systems, University of Duisburg-Essen, Germany, Publisher Shaker-Verlag ISBN: OND-00000-0000093, 2011

VI. APPENDIX

States and Output Matrices

```
A =
         0    1.0000         0         0
   68.1749         0   12.0773         0
         0         0         0    1.0000
  -54.7168         0 -117.0404         0
B =
      0      0
    2.0205   0
      0      0
      0    -13.0045
C =

     1     0     0     0
     0     0     1     0
```

Augmented States Matrix

```
AA =
         0    1.0000         0         0         0
   68.1749         0   12.0773         0    2.0205
         0         0         0    1.0000         0
  -54.7168         0 -117.0404         0  -13.0045
         0         0         0         0         0
```

Compensator and Estimator gain matrices

```
K =
   47.9491    5.5072    4.7672   -0.2978
L1 =
   1.0^+04x

    0.0095
    0.3545
   -0.0426
    1.9657
    3.0760
```

Here, L1=[La ;Ld] where La estimates the system states and Ld estimates the disturbances states. The first 4x1 is La and the last 1x1 is Ld)